Journal of Environmental Chemical Engineering 8.2 (2020): 103689

DOI: https://doi.org/10.1016/j.jece.2020.103689

Revised manuscript submitted to
Journal of Environmental Chemical Engineering
October 2019

Improving the activity in hydrodechlorination of Pd/C catalysts by nitrogen doping of activated carbon supports

C. Ruiz-Garcia[1,2]*, F. Heras[1], L. Calvo[1], N. Alonso-Morales[1], J.J. Rodriguez[1], M.A. Gilarranz[1]

[1]Departamento de Ingeniería Química, Universidad Autónoma de Madrid, Spain.
[2]POR2E Group, CEMHTI (UPR 3079) CNRS, Univ. Orleans, France *(Present address)*

KEYWORDS

Nitrogen doped carbon, activated carbon, hydrodechlorination

ABSTRACT

Aqueous phase 4-chlorophenol hydrodechlorination reaction was used to study the effect of N-doping of activated carbon support on the catalytic activity of Pd catalysts. Activated carbon was doped using pyridine and 1,10-phenantroline, reaching nitrogen contents of 0.42-1.22 and 1.35-4.19 % (w), respectively. All catalysts (0.75% Pd w, carbon basis) showed relatively large Pd nanoparticles (35-55 nm), but they exhibited fast and complete 4-chlorophenol disappearance in batch experiments. In runs at 30 ^{o}C 4-chlorophenol disappearance was mainly ascribed to hydrodechlorination, although N-doping of the support also increased adsorption. Catalysts with supports doped with pyridine yielded higher 4-chlorophenol disappearance rate in spite of lower bulk nitrogen content, however they showed higher concentration of nitrogen species at the external surface and lower loss of surface area during the doping. 4-chlorophenol disappearance rate was boosted at 60 ^{o}C, with minor differences between catalysts with undoped and N-doped support, but generation of cyclohexanone was only observed for the ones with doped support. Phenol generation simultaneous to 4-chlorophenol disappearance was observed with all the catalysts. However subsequent hydrogenation to cyclohexanone ocurred only with the catalysts supported on N-doped activated carbon.

1. INTRODUCTION

Hydrodechlorination is a low-energy technology capable of transforming chlorinated organics into less harmful and toxic products [1-3]. Hydrodechlorination of chlorophenols is a reaction catalyzed in advantageous conditions by metals [4] and showing high sensitiveness to the structure of metal phase and supports [5-7]. Different supports for metal catalysts including activated carbon, silica, alumina, zeolite and mesoporous materials, have been reported for hydrodechlorination [8-10], but carbon materials, especially activated carbons (ACs), are frequently used because of their chemical resistance, well-developed surface tunable porous texture, modifiable surface chemistry, high availability and relatively low cost [11-14].

Improving the hydrodechlorination catalysts performance is crucial in order to achieve process intensification and maximize detoxification, together with stability. Previous works have proved that performance of carbon-based hydrodechlorination catalysts is dependent largely on support properties [4-6, 15]. Likewise, some works have reported higher activity for catalysts supported on N-doped graphene and bulk N-doped carbons [16-18].

Surface chemistry of carbon materials is particularly relevant for catalyst performance, since it contributes to dispersion and stability of active phase, and also can play a role in the reaction mechanism [13, 19, 20]. Thus, Pd and Pt catalysts supported on porous carbons can be reused and exhibit a high stability during hydrodechlorination of chlorophenols in water, showing no changes in nanoparticle size and structure and not measurable metal leaching [4,21]. Even with more complex matrices, results obtained from three-cycle experiments indicated that Pd/C catalysts have a good potential for removing chlorinated compounds [41]. This type of catalysts also exhibited a high stability in continuous experiments, without significant loss of activity after 100 h on stream once the steady-state was reached [54]

One of the methods for chemical structure modification of carbon materials that has received more attention in the last years is doping. This method consists in the introduction of heteroelements into the carbon matrix, either by substitution of C atoms by heteroatoms, or by generation of surface functional groups containing heteroatoms [22-24]. Several studies showed that modification of carbon matrix with different electron

donor or acceptor elements, mainly N, P, B and O, but also S and other elements, increases electrochemical and catalytic performance by modification of electronic properties and surface functional groups of carbon materials [25,26].

Nitrogen is by far the most studied element in carbon doping. Nitrogen is adjacent to carbon in the periodic table and shows important similarities to it. Close atomic radius and electrons number make relatively easy substitution of carbon atoms by nitrogen [27]. Nitrogen atoms introduce basic sites, increasing surface polarity and electron-donor properties of carbon. Changes in chemical structure and electronic properties conferred by N-doping make possible to use them as catalysts or as active phase supports with improved characteristics [25].

When carbon materials are doped with nitrogen, this element is mostly found as pyridinic and pyrrolic groups, but other groups are also formed in variable amounts, such as N-quaternary, pyridine oxide, amine, etc. [28-29]. Some authors indicate that C-N bonds and nitrogen groups behave as active sites for nucleation and growth of active metal particles. Likewise, binding energy between carbon and metal nanoparticles are higher for N-doped than for non-doped carbons, improving metal stability [19, 30]. Binding between metal nanoparticles and N-doped carbon can also favor charge transfer thus modifying acid-base properties [29, 31]. The changes in chemical composition of N-doped carbons used as catalyst supports also can influence the interaction with reagents and reaction products in the liquid phase [32].

Doping has shown positive effects for adsorption and catalysis [27, 33-35], and applications have been extended to a variety of fields [36] including supercapacitors [37, 38], fuel cells [39], photocatalysis [40] sensors/biosensors [41], etc. Doping by simultaneous introduction of more than one element has also been reported [27]. A high stability has been observed for carbon-supported catalysts even in cases where nanoparticles were formed by chemical reduction [42], without conducting a precursor calcination step. N-doping can be expected to confer additional anchorage sites to Pd phase avoiding agglomeration and leaching [43,44]. Likewise, N-doped carbon supports showed negligible changes in N species distribution during hydrodechlorination reactions [4].

Although there is no consensus on the N-groups playing major role in catalytic performance, it is generally accepted that changes in structure and electronic properties modify the activity of catalysts supported on N-doped carbons for different reactions (such

as reductions), due to the net positive charge of carbon atoms adjacent to nitrogen caused by its electron acceptor characteristics. He et al. (2016) [29] and Liu et al. (2015) [25], reported improved results with catalysts supported on N-doped carbons including pyridinic, and graphitic nitrogen groups. In any case, the benefits of N-doping different carbonaceous materials used as metallic catalysts supports have been proved in a diversity of reactions. Important attention has been received by Pd catalysts supported on N-doped carbons, with applications that include perchlorate reduction [32], aniline oxidation [45], chemoselective hydrogenations [31, 46] or hydrodechlorination [4, 15-17].

In general, two main methodologies can be considered for N-doped carbon materials preparation: i) direct synthesis by pyrolysis of nitrogen-containing carbon precursor, or nitrogen and carbon precursors mixtures, and ii) doping of starting carbon material with nitrogen-containing agents. This second alternative allows selecting a starting carbon material with desired textural properties and chemical composition or with other characteristics interesting for application. In the case of ACs, they are widely used as catalytic supports because of their convenient porous texture. ACs N-doping allows additional tailoring of chemical properties, thus expanding the application range and enabling optimized catalysts preparation. In most cases, ACs N-doping consists in carbon impregnation with a doping agent followed by thermal treatment, or CVD deposition on starting carbon using a doping agent as precursor [47].

In the current study, aqueous phase 4-chlorophenol (4-CP) hydrodechlorination reaction was selected to evaluate the effect of AC N-doping on the catalytic activity of carbon-supported Pd catalysts.

2. MATERIALS AND METHODS

2.1. Preparation and characterization of supports and catalysts

N-doped ACs were prepared using a commercial powdered AC (CAPSUPER, Norit) with a particle size smaller than 1 µm. The starting AC was doped with two different N precursors, pyridine and 1,10-phenantroline, in a furnace at 700-900 ^{o}C for 1-3 h in N_2 atmosphere. In N-doping with pyridine, 1 g of starting AC was placed in a furnace and inlet N_2 flow was saturated in pyridine at 40 ^{o}C. In the case of 1,10-phenantroline, 1 g of starting AC was impregnated with a solution of 1,10-phenantroline (0.1 g) in 40 mL of acetone. Then the impregnated AC was subjected to thermal treatment as indicated above. Table 1 summarizes the conditions of N-doping and the samples designation.

Table 1. Operating conditions for the preparation of N-doped ACs.

Sample	Doping agent	Thermal treatment	
		Temperature (ºC)	Time (h)
Py700-1	Pyridine	700	1
Py700-3			3
Py900-1		900	1
Py900-3			3
Ph700-1	1,10-Phenantroline	700	1
Ph700-3			3
Ph900-1		900	1
Ph900-3			3

Starting and N-doped ACs were used as supports for Pd catalysts preparation by incipient wetness impregnation (0.75% w Pd, AC basis) using a solution of $PdCl_2$. A solution volume to the pore volume ratio of 1.3 was used. The impregnated supports were dried overnight at 65 ºC, calcined at 200 ºC for 2 h in air and reduced at 100 ºC for 1 h under continuous H_2 flow of 40 mL·min^{-1}.

2.2. Characterization of catalysts

The materials prepared were characterized by Elemental Analysis (LECO CHNS-932), N_2 adsorption-desorption at 77 K (Micromeritics Tristar II) and Transmission Electron Microscopy (TEM) with a JEOL JEM 2100 apparatus. Porous texture parameters were determined from N_2 adsorption-desorption isotherms using BET, BJH and t-plot methods for specific surface area, mean pore size and micropore volume, and external specific surface, respectively. Transmision electron microscopy (TEM) was used to characterize the structure and morphology of supports and active phases. The average size of the Pd NPs was analyzed and calculated using the J-image software, considering at least 100 nanoparticles from different TEM images, and calculating the average diameter as: $d\bar{t}$=(Σ$i\ nidi$3Σ$i\ nidi2/$)·100 [50]. Catalyst were named with "Pd/" followed by the supports name.

2.3. Hydrodechlorination tests

The catalysts prepared were evaluated in 4-CP hydrodechlorination in water at 30 and 60 °C. Reaction experiments were carried out in a spherical glass-made batch reactor equipped with temperature control, using the following experimental conditions: 800 rpm magnetic stirring, 50 NmL·min^{-1} H_2 flow, 150 mL reaction volume, 100 mg·L^{-1} (0.778 mM) 4-CP initial concentration and 0.77 mg_{Pd}.L^{-1}. Concentration of compounds in the liquid phase was

expressed in mmol/L, since each mol of 4-CP converted results in 1 mol of phenol, which in turn can be partially converted to cyclohexanone [4], thus making easier to follow the mass balance. Reaction monitoring was performed by collecting homogeneous samples of 1.2 mL at different times. Total collected volume was lower than 15 mL. Collected samples were filtered and analyzed by GC-FID (GC 3900 Varian) using a capillary column (CP-Wax 52 CB, Varian) and N_2 as carrier gas. No detectable stripping of 4-CP or reaction products was observed. Likewise, Pd leaching from catalysts was also below TXRF detection threshold.

The catalysts were compared in terms of 4-CP disappearance rate, which was calculated from the pseudo-first-order kinetic constant (*k*) and normalized considering the Pd concentration in the reaction medium, as indicated in Equation 1. Normalized apparent rate (*a*) was used to reflect mmol of 4-CP removed per minute and per unit mass of Pd. This approach was adopted to make possible the comparison of catalysts tested using different concentration of Pd (C_{Pd}) or 4-CP ($C_{4\text{-}CP_0}$) in the reaction medium.

$$a\ (\mathrm{mmol}/\ \mathrm{g}_{Pd}\ \cdot min) = k \cdot \left(C_{\ 4-CP_0}/C_{Pd}\ \right) \qquad (1)$$

3. RESULTS AND DISCUSSION

3.1. Characterization of catalysts

Table 2 shows the elemental analysis of the supports prepared. The starting AC contained some nitrogen (0.29%, w) ascribable to biomass origin, which must be taken into account to analyze the doping level achieved. As it can be observed, the amount of nitrogen inserted in doped ACs was higher with 1,10-phenantroline (3.15-4.19%, w) than with pyridine precursor (0.42-1.35%, w). Both the polyaromatic nature of 1,10-phenantroline and the doping procedure used with this precursor (AC was impregnated with phenantroline) can lead to a higher interaction with the AC [17]. The doping levels achieved with 1,10-phenantroline were higher at 700 than at 900 ^{o}C (4.2 and 3.2% w, respectively), whereas no significant differences were observed at different thermal treatment time. With pyridine slight differences in doping extent were observed between 700 and 900 ^{o}C. However, at both temperatures nitrogen content in AC increased with treatment time because pyridine was incorporated to the reactor throughout the experiment together with the inert gas flow. The carbon content was slightly higher for carbons doped with 1,10-phenantroline, indicating also some deposition of carbon. On the other hand, it is possible to consider that the ratio between the non-quantified elements and C is closely related to O/C ratio, since the ash content is essentially the same for all samples and the rest of elements are in a low concentration. Therefore, a decrease of O/C

ratio can be inferred and ascribed to loss of oxygenated functional groups upon heating and reaction with the doping agents.

Table 2. Elemental analysis of N-doped ACs (%, w).

	C	H	N	Others*
AC	79.95	2.58	0.29	17.18
Py700-1	87.13	1.70	0.71	10.46
Py700-3	86.49	1.47	1.22	10.82
Py900-1	87.72	1.03	0.42	10.83
Py900-3	89.60	0.92	1.35	8.13
Ph700-1	85.51	1.95	4.19	8.35
Ph700-3	86.54	1.58	4.15	7.73
Ph900-1	85.93	1.02	3.16	9.89
Ph900-3	88.25	1.09	3.15	7.51

**By difference (includes ash, oxygen, phosphorus and other minor elements)*

Surface elemental composition of selected samples was analyzed by XPS (Table 3). Compared with the corresponding bulk elemental analyses, the doped ACs obtained with pyridine contain significantly higher concentration of nitrogen on the surface than in bulk carbon. The difference is more pronounced in samples prepared at 900 °C. Heterogeneous distribution of nitrogen in carbons doped using pyridine was also observed in previous works [17]. In N-doped ACs obtained with 1,10-phenantroline more homogeneous distribution of N was found. Therefore, impregnation with precursor solution in acetone can favor penetration into the internal porosity of AC.

Table 3. Surface elemental composition of representative N-doped ACs by XPS (%, w).

	C	N	O
Py700-3	89.5	1.8	8,7
Py900-3	88.9	4.4	6.6
Ph900-3	89.3	2.2	8.5

XPS profiles of nitrogen (405−397 eV range) can be seen in Figure 1. N 1s spectra of ACs Py700-3, Py900-3 and Ph900-3 were deconvoluted in order to identify nitrogen bonding configurations. Peak position and percentage of each nitrogen bonding species are summarized in Table 4. The main contribution to XPS nitrogen signal is associated with two nitrogen configurations, pyridinic-N at 398.3 eV and quaternary at 401.4 eV, with percentages of 23.9-25.4% and 21.7-28.2%, respectively. Pyrrolic contribution is also important, especially

in the case of Ph900-3 (28.3%). Quaternary and pyridinic-N atomic ratios (Q-N/P-N) were similar in all samples, with much lower relative significance (0.9-1.2%).

Table 4. Deconvolution of XPS N 1s signal of N-doped ACs spectra.

	Reference Peak position*	Py700-3 Peak position	Area (%)	Py900-3 Peak position	Area (%)	Ph900-3 Peak position	Area (%)
Pyridinic-N (P-N)	398-398.3	398.3	24.5	398.3	23.9	398.3	24.3
Aminic-N (A-N)	399.0	399.5	7.6	399.4	12.0	399.5	13.6
Pyrrolic-N (Py-N)	400-400.1	400.6	16.8	400.5	21.9	400.5	28.3
Quaternary (Q-N)	400.7-401.5	401.4	21.7	401.4	28.2	401.5	26.7
Pyridinic oxides (P-O)	402-403	402.7	20.3	402.8	9.5	402.8	7.1
N_2 (N)/N-oxides (O-N)N-	404-405	405.8	8.7	405.5	4.6	---	---
(Q-N)/(P-N) ratio		0.9		1.2		1.1	

*[23, 51]

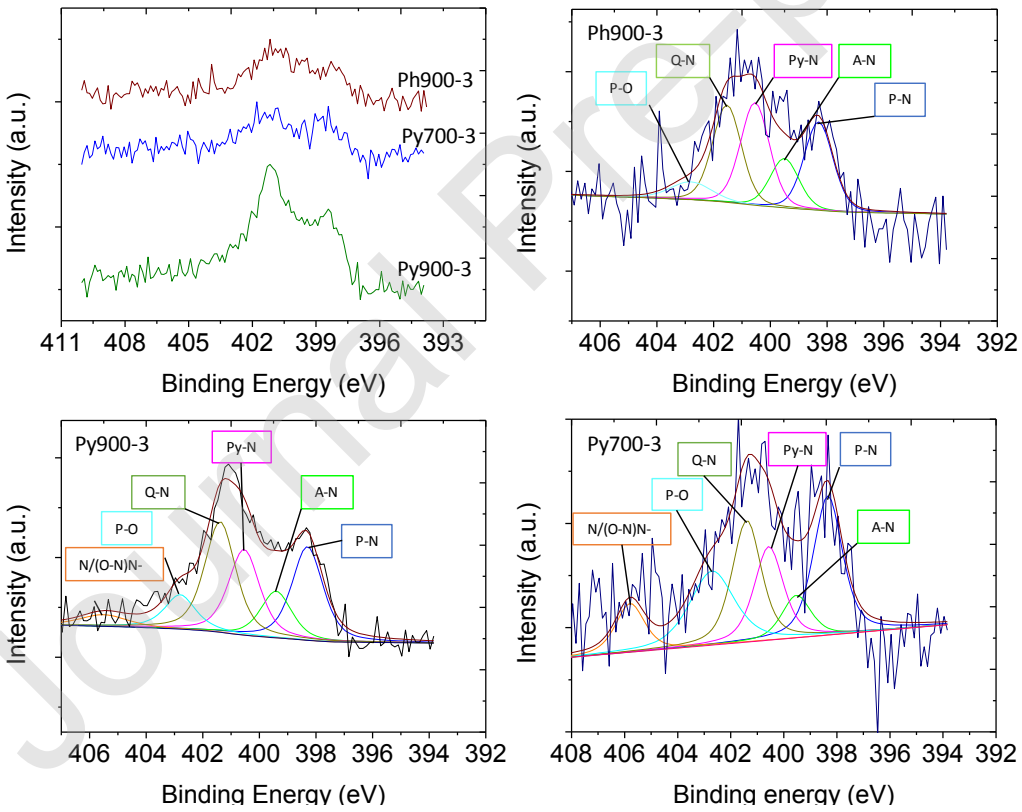

Figure 1. N 1s XPS spectra of N-doped ACs prepared with pyridine and 1,10-phenantroline and deconvoluted curves.

As can be observed in Table 5, carbons doped with pyridine and treated for 1 h exhibited textural properties close to those of starting AC, showing that pyrolytic carbon and nitrogen

inclusion had minor effect on surface area and pore volume. However, when samples were treated during 3 h a noticeable decrease in S_{BET} and external or non-micropore area was observed (around 30%). Doping with 1,10-phenanthroline led to an important decrease of surface area and pore volume, with very low influence of treatment temperature and time. Micropores blockage can be inferred from the important drop of micropore volume and the increase of mean pore size. These results are consistent with the higher insertion of nitrogen achieved with this doping agent.

Table 5. Porous texture of N-doped ACs.

	S_{BET} (m^2/g)	A_{EXT} (m^2/g)	V_{meso} (cm^3/g)	V_{micro} (cm^3/g)	d_{BJH} (nm)
AC	1600	682	0.72	0.320	3.7
Py700-1	1339	705	0.66	0.320	3.7
Py700-3	1031	485	0.51	0.250	3.7
Py900-1	1514	649	0.68	0.400	3.7
Py900-3	1032	481	0.51	0.250	3.8
Ph700-1	570	398	0.44	0.072	4.5
Ph700-3	600	397	0.43	0.086	4.4
Ph900-1	543	353	0.38	0.081	4.3
Ph900-3	593	394	0.42	0.084	4.3

TEM was used to characterize the catalyst metallic phase (Figure 2). All samples showed pseudospherical metal nanoparticles well distributed on the support. A wide nanoparticle size range can be observed in all the cases, with relatively high mean values ranging between 33 and 54 nm. The doping conditions do not seem to affect significantly to the mean Pd nanoparticle size although the catalysts supported on carbons doped using pyridine showed nanoparticles with slightly larger mean size. Attending to the nanoparticle size distributions, equivalent metallic phase dispersion can be assumed for all catalysts prepared. XPS analysis of Pd showed a Pd content on ACs surface around 0.8% w, which is similar to the nominal Pd content and indicates homogenous distribution of the metallic phase on the catalyst support. This is a good starting point for the comparison of their performance. In addition, no important differences in morphology can be observed between the starting and doped ACs, although Py900-3 shows more defined contours probably due to deposition of pyrolytic carbon on the outermost surface.

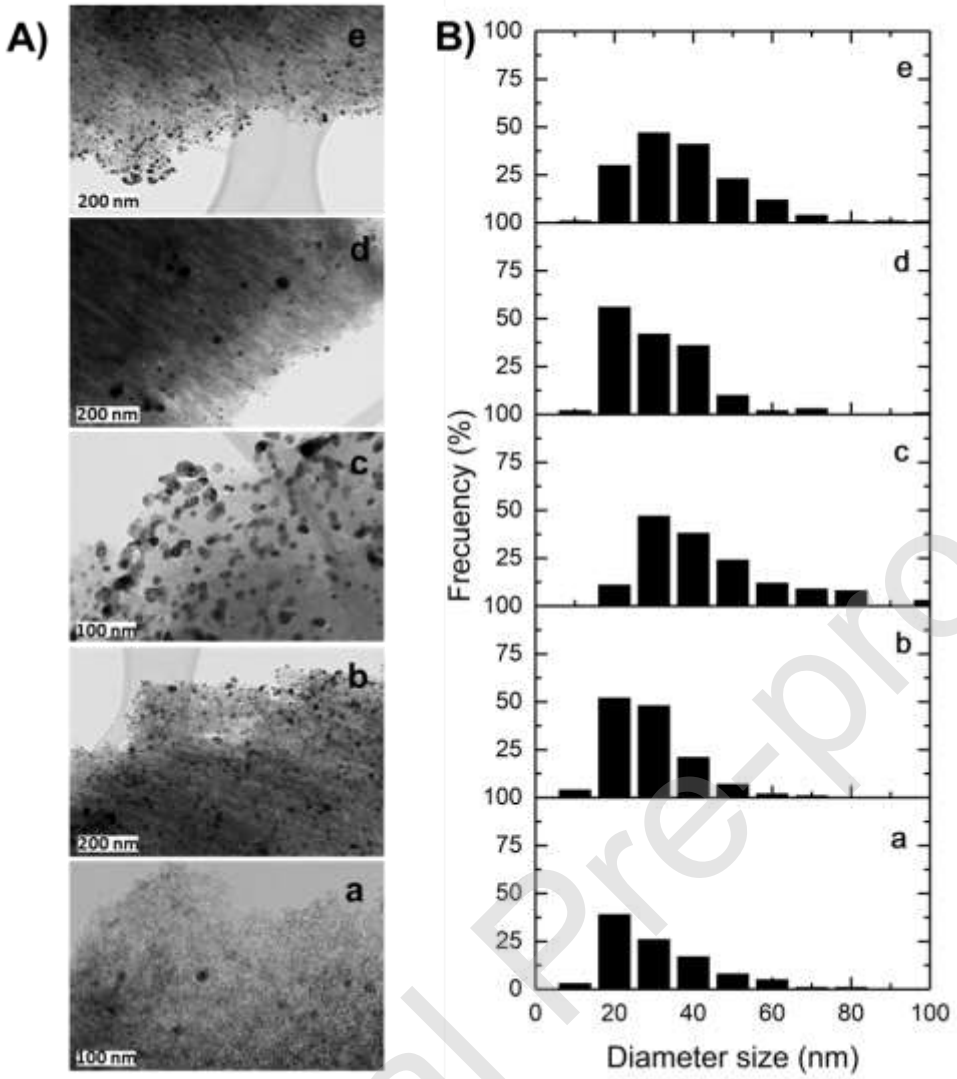

Figure 2. A) Representative TEM images of selected catalyst samples and B) Pd nanoparticle size distributions, from the a) Pd/AC, b) Pd/PY700-3, c) Pd/PY900-3, d) Pd/PH700-3, e)Pd/PH900-3 catalysts

3.2. Catalyst testing in 4-CP hydrodechlorination

Two series of experiments were carried out to evaluate the activity of the Pd catalysts prepared with N-doped carbons as supports in 4-CP hydrodechlorination. All catalysts prepared were tested at 30 ^{o}C, and then a selected set of catalysts was also tested at 60 ^{o}C. As can be observed in Figure 3, in the experiments at 30 °C 4-CP was completely removed after 30 min of reaction time with all catalysts tested. Simultaneous and fast appearance of phenol shows evidences 4-CP removal by hydrodechlorination is responsible for most of the removal, although the incomplete closure of mass balance suggests some adsorption of 4-CP and/or

reaction products. Other works have shown that catalysts supported on highly porous carbons exhibited a relevant contribution of adsorption in hydrodechlorination experiments [52,53], and the difficulty to decouple 4-CP hydrodechlorination and adsorption, also affecting mass balance closure [52-54]. Some of the activation energy values reported in literature for 4-CP hydrodeclorination using Pd and Pt catalysts supported on porosus materials are in the 15-36 kJ·mol-1 range [4,55], which has been related to important significant contribution of physical phenomena, particularly adsorption, since some a minor mass transfer constrains were observed. In a previous work, lower values of apparent activation energies in 4-CP hydrodechlorination were obtained in 4-CP hydrodechlorination with observed for Pd catalysts supported on N-doped porous carbons, together with faster 4-CP removal and less complete mass balance clousure, suggesting a higher contribution of adsorption with these supports [56].

The catalyst supported on the starting AC (non-doped) yielded phenol as the only reaction product detected. However, catalysts supported on N-doped carbon showed some activity in further hydrogenation of phenol, and cyclohexanone was produced at reaction times beyond 30 min. Selectivity to cyclohexanone, here defined as percentage (mole) in the reaction products detected, reached 6-13%. A slightly higher selectivity towards cyclohexanone was observed for catalysts supported on carbons doped using phenanthroline, particularly when doping was carried out at 700 ^{o}C.

Results in the literature show that fairly different selectivities to reaction products have been achieved in 4-CP hydrodechlorination with different catalytic systems based on Pd, and the characteristics of carbon supports seem to play an important role. Unsupported Pd nanoparticles yielded complete conversion of 4-CP into phenol, but they were unable to hydrogenate phenol [6]. Likewise, total selectivity to phenol was observed with Pd catalysts supported on sepiolite-carbon nanocomposites [57], carbon blacks [16] and reduced graphene oxide [7]. On the contrary, relevant selectivity to cyclohexanol and cyclohexanone was observed with Pd supported on ACs with different contents of oxygen surface groups [58,59] and on N-doped-ordered mesoporous carbons [60]. In addition, selectivity to cyclohexanone can be boosted by alkali addition, using Pd supported on activated carbon [61] or graphene [10], and with Pd-Sn/C bimetallic catalysts [62].

XPS spectra of the Pd 3d region (Figure 4) show that Pd^{n+}/Pd^{0} ratio was around 1.0 for the catalyst prepared from ACs doped with pyridine and with phenanthroline. The presence of the

two Pd species has been reported to contribute to catalytic activity, being favored at ratios around 1.0 [63].

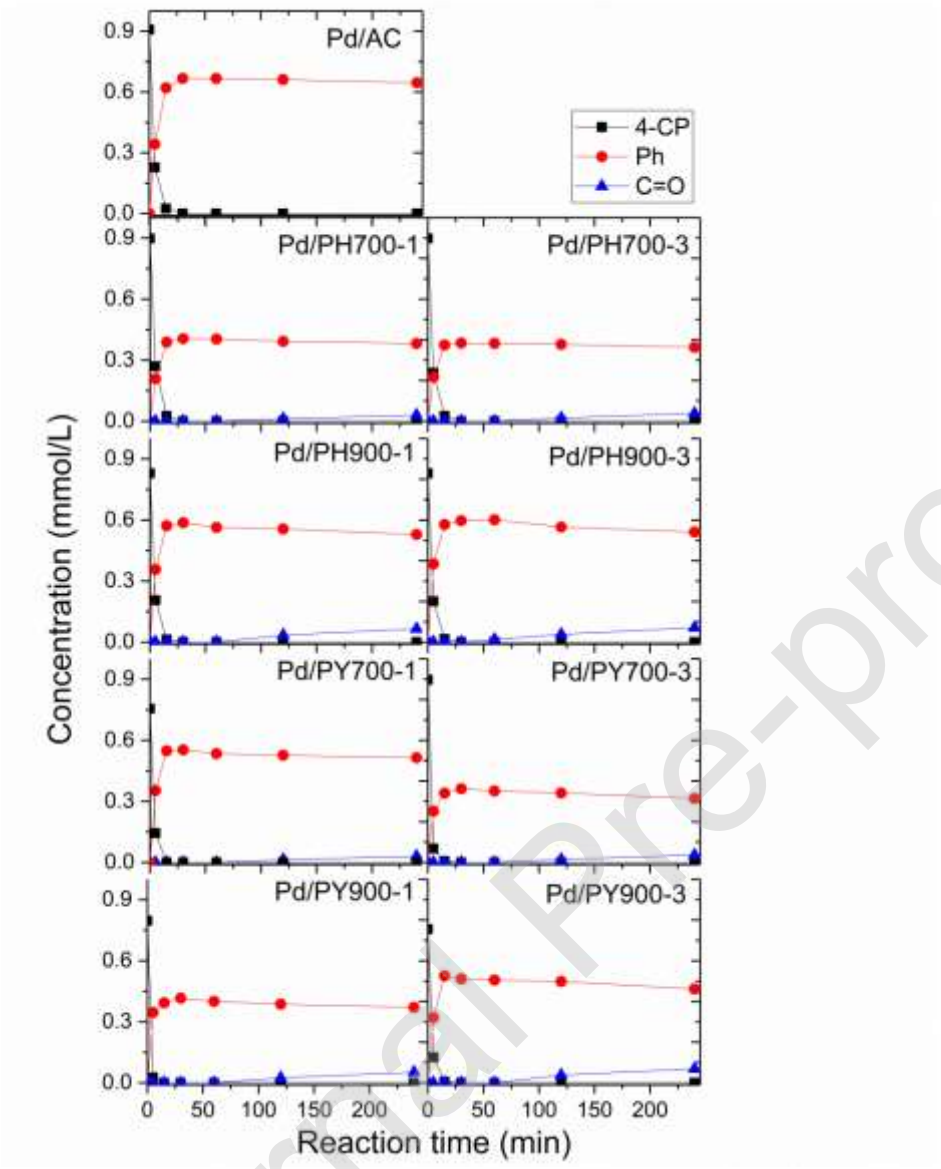

Figure 3. Time-course of 4-CP normalized molar concentration and reaction products upon hydrodechlorination tests at 30°C.

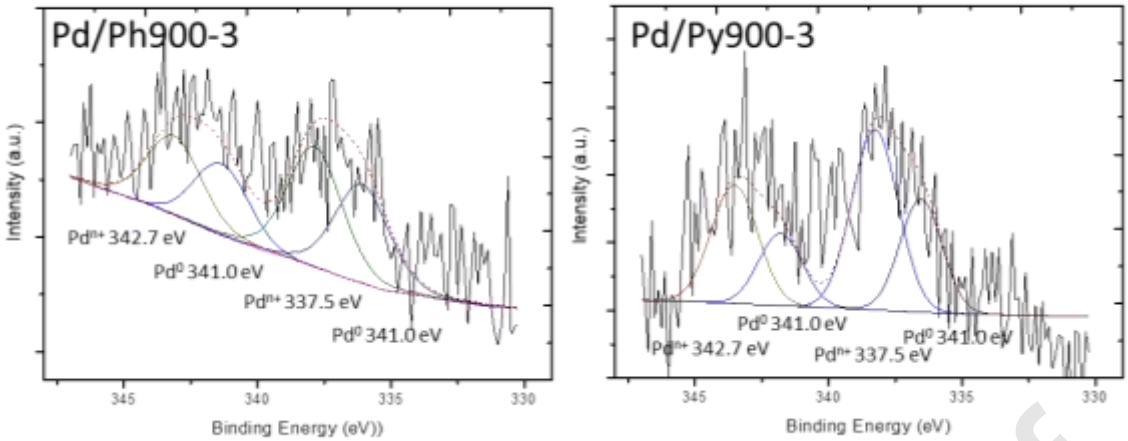

Figure 4. Deconvoluted XPS spectra of Pd 3d for catalyst prepared from AC doped with pyridine (Py900-3) and 1,10-phenantroline (Ph900-3).

Values of pseudo-first order kinetic constant for 4-CP disappearance and normalized apparent rate were calculated (Table 6) from data of Figure 3. As a general trend, the catalysts prepared with N-doped AC supports yielded faster 4-CP disappearance than the one prepared with the undoped starting AC. Likewise higher values were found for the catalyst with supports doped with pyridine, which could be related with the higher surface area of those carbon supports and to preferential N-doping at the external surface. Therefore, for this set of materials the location of the N species and the surface area is more determining than the total amount of N incorporated. The run with catalyst Pd/Py900-1 yielded significantly higher 4-CP disappearance rate (200 mmol/g_{Pd}·min). The support for this catalyst has the lowest nitrogen among doped ACs, and hence the highest surface area. In spite of the fast 4-CP disappearance the generation of phenol is rather low compared to other catalysts. This behavior suggests that adsorption of 4-CP and/or phenol may be relevant for Pd/Py900-1 and the high apparent rate observed may include that contribution. Interestingly, disappearance rate with Pd/Py900-1 is faster than with Pd/AC, indicating that doping must affect to both 4-CP adsorption and hydrodechlorination.

Table 6. Kinetic values calculated form 4-CP hydrodechlorination tests at 30 °C.

	k (min^{-1})	R^2	a ($mmol/g_{Pd}·min$)	Mass balance closure (%)
Pd/AC	0.24	0.997	87	98
Pd/Py700-1	0.30	-	100	72
Pd/PY700-3	0.27	0.977	97	39
Pd/Py900-1	0.60	-	200	53
Pd/Py900-3	0.32	0.998	97	70
Pd/Ph700-1	0.27	0.995	96	46
Pd/Ph700-3	0.33	0.970	116	45
Pd/Ph900-1	0.28	0.999	93	72
Pd/Ph900-3	0.27	0.999	89	74

Additional 4-CP hydrodechlorination experiments were carried at 60 °C. At this temperature the contribution of adsorption is expected to be much lower, as it has been found in a number of works dealing with adsorption of 4-CP and phenol on porous carbons [64-66]. Likewise, Pd/AC was compared at 60 °C to the Pd/Py900-3 and Pd/Ph900-3 catalysts, as they showed similar 4-CP removal rates at 30 °C and higher mass balance closure indication lower contribution of adsorption. The results in Figure 5 show a dramatic increase of 4-CP disappearance by increasing the reaction temperature up to 60 °C. Complete 4-CP removal was achieved in a reaction time shorter than 15 min. A slightly faster 4-CP disappearance can be observed for Pd/AC. Figure 5 also shows simultaneous and very fast generation of phenol. As in the case of the experiments at 30 °C, at 60 °C phenol was the only reaction product detected in the reaction with AC/Pd, whereas selectivity towards cyclohexanone for Pd/PH900-3 and Pd/Py900-3 increased to 22 and 32%, respectively. However the increase of hydrogenation activity was much lower that of hydrodechlorination.

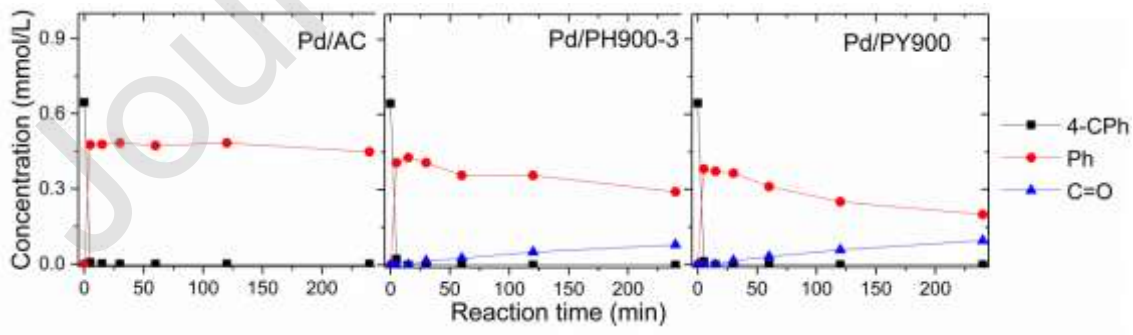

Figure 5. Results of hydrodechlorination tests at 60 °C for selected catalysts.

4. CONCLUSIONS

N-doped carbons have been obtained from a commercial activated carbon using pyridine and 1,10-phenanthroline as nitrogen precursors. The type of precursor and doping conditions determined different nitrogen contents in the doped activated carbons, with pyridine leading to lower bulk nitrogen content but with preferential concentration at the external surface.

The catalysts prepared with N-doped carbons exhibited large Pd nanoparticles in the 35-55 nm range, although all of them showed a higher activity in 4-CP hydrodechlorination, than the one supported on the undoped carbon. Also, some cyclohexanone was produced upon further hydrogenation of phenol. Nitrogen doping of the support clearly increased 4-CP disappearance rate, especially with pyridine as doping agent. N-doping of the carbon support seem also lead to higher contribution of adsorption to 4-CP removal. Increasing reaction temperature from 30 to 60 ^{o}C resulted in an increase of 4-CP disappearance rate. At 60 ^{o}C differences between catalysts with non-doped and doped support were very low, but only those with doped support yielded cyclohexanone.

Declaration of interest statement:

None

Sample CRediT author statement

C. Ruiz-Garcia: Conceptualization, Methodology, Formal analysis, Investigation, Writing - Original Draft, Writing - Review & Editing; **F. Heras**: Conceptualization, Methodology, Writing - Original Draft; **N. Alonso-Morales**: Formal analysis, Investigation, Writing - Review & Editing; **L. Calvo**: Methodology, Writing - Review & Editing, Project administration, Funding acquisition; **J.J. Rodriguez**: Conceptualization, Writing - Review & Editing; **M.A. Gilarranz**: Conceptualization, Methodology, Writing - Review & Editing, Project administration, Funding acquisition

ACKNOLEDGEMENTS AND FUNDING SOURCES

The authors greatly appreciate the financial support of this research from the Spanish Ministry of Economy and Competitiveness through the project CTQ2012-32821 and C. Ruiz-García for PhD grant (BES-2013-06608 5).

REFERENCES

[1] Pizarro, A.H.; Molina, C.B.; Munoz, M.; de Pedro, Z.M.; Menendez, N.; Rodriguez J.J. App. Catal. B: Environ. 2017, 216, 20–29

[2] Wu, B.-Z.; Chen, H.-Y.; Wang, S.J.; Wai, C.M.; Liao, W.; Chiu, K. Chemosphere. 2012, 88, 757-768.

[3] Xiong, J.; Ma, Y.; Yang, W.; Zhong, L. J. Hazard. Mater. 2018, 355, 89-95.

[4] Ruiz-García, C.; Heras, F.; Calvo, L.; Alonso-Morales, N.; Rodriguez, J.J.; Gilarranz, M.A. App. Catal. B: Environ. 2018, 238, 609-617

[5] Diaz, E.; Casas, J.A.; Mohedano, A.F.; Calvo, L.; Gilarranz, M.A.; Rodriguez, J.J. Ind. Eng. Chem. Res. 2009, 48, 3351–3358.

[6] Baeza, J.A.; Calvo, L.; Gilarranz, M.A.; Mohedano, A.F.; Casas, J.A.; Rodriguez, J.J. J. Catal. 2012, 293, 85-93

[7] Deng, H.; Fan, G.; Wang, C.; Zhang, L. Catal. Commun. 2014, 46, 219–223.

[8] Gómez-Quero S.; Cárdenas-Lizana F.; Keane M.A. Ind. Eng. Chem. Res., 2008, 47,6841-6853

[9] Munoz, M.; de Pedro, Z.M.; Casas, J.A.; Rodriguez, J.J. Appl. Catal. A, 2014, 488, 78-85

[10] Chang, W.; Kim, H.; Oh, J.; Ahn, B.J. Res. Chem. Intermed. 2018, 44, 3835–3847.

[11] Figueiredo, J.L.; Pereira, M.F.R.; Freitas, M.M.A., Órfão, J.J.M. Carbon 1999, 37, 1379-1389.

[12] Fidalgo, B.; Zubizarreta, L.; Bermúdez, J.M.; Arenillas, A.; Menéndez, J.A. Fuel Process. Technol. 2010, 91, 765-769.

[13] Prati, L.; Villa, A.; Chan-Taw, C.E.; Arrigo, R.; Wang, D.; Su, D.S. Faraday Discuss. 2011, 152, 353-365.

[14] Diaz, E.; Mohedano, A.F.; Casas, J.A.; Calvo, L.; Gilarranz, M.A.; Rodriguez, J.J. Appl. Catal. B, 2011, 106, 469-475

[15] Ruiz-García, C.; Heras, F.; Alonso-Morales, N.; Calvo, L.; Rodriguez, J.J.; Gilarranz, M.A. Catal. Sci. Technol. 2018, 8, 2598-2605.

[16] Baeza, J.A.; Alonso-Morales, N.; Calvo, L.; Heras, F.; Rodriguez, J.J., Gilarranz, M.A. Carbon 2015, 87, 444-52

[17] Alonso-Morales, N.; Ruiz-García, C.; Heras, F.; Calvo, L.; Alonso-Morales, N.; Rodriguez, J.J.; Gilarranz, M.A.2017. Ind. Eng. Chem. Res. 2017, 56, 7665-74.

[18] Zhou, J.; Chen, Q.; Hanb, Y.; Zheng, S. RSC Adv. 2015,5, 91363-91371

[19] Arrigo R.; Schuster M.E.; Xie Z.; Yi Y.; Wowsnick G.; Sun L.L.; Hermann K.E.; Friedrich M.; Kast P.; Hävecker M.; Knop-Gericke A.; Schlögl R. ACS Catal. 2015, 5(5), 2740-53.

[20] García, R.; Soto, G.; Escalona, N.; Sepúlveda, C.; Orellana, M.J.; Morales, N.; Radovic, L.R.; Buitrago-Sierra, R.; Rodriguez-Reinoso, F.; Sepúlveda-Escribano, A. Quim. Nova 2015, 38(4), 506-509.

[21] Calvo, L.; Gilarranz, M.A.; Casas, J.A.; Mohedano, A.F.; J. Hazard. Mater., 2009, 161, 842–847

[22] Maldonado, S.; Stevenson, K.J. J. Phys. Chem. B 2005, 109, 4707-4716.

[23] Inagaki, M.; Toyoda, M.; Soneda, Y.; Morishita, T. Carbon 2018, 132, 104-140.

[24] Ha, S.; Choi, G.B.; Hong, S.; Kim, D.W.; Kim, Y.A. carbon Lett. 2018, 27, 1-11.

[25] Liu, L.; Zhu, Y.-P.; Su, M.; Yuan, Z.-Y. ChemCatChem 2015, 7, 2765-2787.

[26]Hulicova-Jurkacova, D.; Kodama, M.; Shiraishi, S.; Hatori, H.; Zhu, Z.H.; Lu, G.Q. Adv. Funct. Mater. 2009, 19, 1800-1809.
[27]Paraknowitsch, J.P; Thomas, A. Energ. Environm. Sci. 2013, 6(10), 2839-55.
[28]Nieto-Marquez, A.; Toledano, D.; Sánchez, P.; Romero, A.; Valverde, J.L. J. Catal. 2010, 269(1), 242-51.
[29]He, L.; Weniger, F.; Neumann, H.; Beller, M. Angew. Chem. Int. Ed. 2016, 55(41), 12582-94.
[30]Wang, Y.; Yao, J.; Li, H.; Su, D. Antonietti, M. J. Am. Chem. Soc. 2011, 133, 2362.
[31]Li, Z.; Liu, J.; Xia, C.; Li, F. ACS Catal. 2013, 3(11), 2440-48
[32]Kim, Y.-N.; Lee, Y.-C.; Choi, M. Carbon 2013, 65, 315-23.
[33]Duan, X.; Indrawirawan, S.; Sun, H.; Wang, S. Catal. Today 2015, 249, 184-91.
[34] Liu, T.; Li, M.; Bo, X.; Zhou, M. J. Colloid. Interf. Sci 2019, 533, 709-722.
[35] Donglin, H.; Zhao, W.; Li, P.; Sun, S.; Tan, Q.; Liu, L.; Liu, L.; Qu, X. J. Alloy. Comp. 2019, 73, 11-20.
[36]Agnoli, S.; Favaro, M. J. Mater. Chem. A 2016, 4, 5002.
[37]Wang, T.; Zhang, J.; Hou, Q.; Wang, S. J. Alloys Comp. 2019, 771, 1009-1017
[38]Deng, Y.; Xie, Y.; Zou, K.; Ji, X. J. Mater. Chem. A 2016, 4(4), 1129-1532.
[39]Shao, Y.; Yin, Y.; Shi, P. J. Electrochem. Soc. 2006, 153(6), A1093-A1097.
[40]Shindume, H.L.; Zhao, Z.Y.; Wang, N.; Liu, H.; Umar, A.; Zhang, J.X.; Wu, T.T., Guo, Z.H. J. Nanosci. Nanotechnol. 2019, 19(2), 839-849
[41]Qin, Z.; Wang, W.; Zhan, X.; Du, X.; Zhang, Q.; Zhang, R.; Li, K.; Li, J.; Xu, W. Spectrochim. Acta A: Molec. Bimolec. Spectrosc. 2019, 208, 162-171.
[42]She, X.; Yang, Q.; Yao, F.; Zhong, Y.; Ren, W.; Chen, F.; Sue, J.; Ma, Y.; Fe, Z.; Wang, D. Chem. Eng. J., 2009, 358, 903-911.
[43]An, N.; Zhang, M.; Zhang, Z.; Dai, Y.; Shen, Y.; Tang, C.; Yuan, X.; Zhou, W. J. Colloid. Interface Sci. 2018, 510, 181-189.
[44]Li, R.; Wang, S.;·Hu, Y.; Chen, H.; Chen, J.; Chu, C., Zheng, J. Chem. Pap. 2018, 72, 2425–2432.
[45]Yan, Y.; Miao, J.; Yang, Z.; Xiao, F.X., Yang, H.B.; Liu, B.; Yang, Y. Chem. Soc. Rev. 2015, 44(10), 3295-346
[46]Deshmukh, A.A.; Islam, R.U.; Witcomb, M. J.; Otterlo, W.A.L.; Coville, N. J. ChemCatChem 2010, 2(1), 51-4
[47]Li, R.; Wang, S.;·Hu, Y.; Chen, H.; Chen, J.; Chu, C., Zheng, J. Chem. Pap. 2018, 72, 2425–2432.
[48]Amorim, C.; Yuan, G.; Patterson, P.M.; Keane, M.A. J. Catal. 2005, 34, 268-281.
[49]Díaz, E.; Ordóñez, S.; Bueres, R.F.; Asedegbega-Nieto, E.; Sastre, H. App. Catal. B: Environm. 2010, 99, 181-190
[50]Krishnankutty, N. and Vannice, M.A. J. Catal. 1995, 2, 312-326
[51]Susi, T.; Pichler, T.; Ayala, P. Beilstein J. Nanotechnol. 2015, 6, 177-192.
[52]Munoz, M.; Kaspereit, M.; Etzold, B.J.M. Chem. Eng. J. 2016, 285, 228-235.
[53]Munoz, M.; Zhang, G.-R.; Etzold, B.J.M. Appl. Catal. B-Environ. 2017, 203, 591-598
[54]Munoz, M.; Kolb, V.; Lamolda, A.; de Pedro Z.M.; Modrow, A.; Etzold, B.J.M.; Rodriguez, J.J.; Casas, J.A. Appl. Catal. B-Environ., 218, 2017, 498-505
[55]Diaz, E.; Casas, J.A.; Mohedano, A.F.; Gilarranz, M.A., Rodriguez, J.J. Ind. Eng. Chem. Res. 2008, 47, 3840-3846
[56]Ruiz-García, C.; Heras, F.; Alonso-Morales, N.; Calvo, L.; Rodriguez, J.J.; Gilarranz, M.A Ind. Eng. Chem. Res., 2019, 58, 4355-4363.

[57]Ruiz-García, C.; Heras, F.; Gilarranz, M.A.; Aranda, P.; Ruiz-Hitzky, E. Appl. Clay Sci. 2018, 161, 132-138.
[58]Calvo, L.; Gilarranz, M.A.; Casas, J.A.; Mohedano, A.F.; Rodriguez, J.J. App. Catal. B: Environ. 2006, 67(1-2), 68-76.
[59]Díaz, E.; Mohedano, A.F.; Casas, J.A.; Calvo, L.; Gilarranz, M.A.; Rodriguez, J.J. App. Catal. B: Environ. 2011, 106(3-4), 469-475.
[60]Li, R.; Wang, S.; Hu, Y.; Chen, H.; Chen, J.; Chu, C.; Zheng, J. Chem. Papers 2018, 72(10), 2425-2432.
[61]Yuan, G.; Keane, M. J. Catal. 2004, 225(2), 510-522.
[62]Fang, X.; Fang, D. RSC Adv. 2017, 7, 40437.
[63]Gomez-Sainero, L.; Seoane, X.; Fierro, J.; Arcoya, A. J. Catal. 2002, 209, 279–288.
[64]Ma, Y.; Gao, N.; Chu, W.; Li, C.; Front. Environ. Sci. Eng. 2013, 7(2), 158-165.
[65]Rincon-Silva, N.G.; Moreno-Pijarán, J.C.; Giraldo Giraldo, L. J. Chem. 2015, Art. ID: 569403.
[66]Sun, J.; Liu, X.; Zhang, F.; Zhou, J.; Wu, J.; Alsaedi, A.; Hayat, T.; Li, JX. Colloids Surf. A 2019, 563, 22-30.